Pi and sigma double conjugations in boronyl polyboroene nanoribbons: B n (BO)2 and B n (BO)2 (n = 512)

Hua-Jin Zhai, Qiang Chen, Hui Bai, Hai-Gang Lu, Wei-Li Li, Si-Dian Li, and Lai-Sheng Wang

Citation: The Journal of Chemical Physics **139**, 174301 (2013); doi: 10.1063/1.4827501
View online: http://dx.doi.org/10.1063/1.4827501
View Table of Contents: http://scitation.aip.org/content/aip/journal/jcp/139/17?ver=pdfcov
Published by the AIP Publishing

THE JOURNAL OF CHEMICAL PHYSICS **139**, 174301 (2013)

Pi and sigma double conjugations in boronyl polyboroene nanoribbons: $B_n(BO)_2^-$ and $B_n(BO)_2$ ($n = 5-12$)

Hua-Jin Zhai,[1,2,a)] Qiang Chen,[1] Hui Bai,[1] Hai-Gang Lu,[1] Wei-Li Li,[2] Si-Dian Li,[1,a)] and Lai-Sheng Wang[2,b)]
[1]*Nanocluster Laboratory, Institute of Molecular Science, Shanxi University, Taiyuan 030006, China*
[2]*Department of Chemistry, Brown University, Providence, Rhode Island 02912, USA*

(Received 15 September 2013; accepted 16 October 2013; published online 1 November 2013)

A series of boron dioxide clusters, $B_xO_2^-$ ($x = 7-14$), have been produced and investigated using photoelectron spectroscopy and quantum chemical calculations. The dioxide clusters are shown to possess elongated ladder-like structures with two terminal boronyl (BO) groups, forming an extensive series of boron nanoribbons, $B_n(BO)_2^-$ ($n = 5-12$). The electron affinities of $B_n(BO)_2$ exhibit a $4n$ periodicity, indicating that the rhombic B_4 unit is the fundamental building block in the nanoribbons. Both π and σ conjugations are found to be important in the unique bonding patterns of the boron nanoribbons. The π conjugation in these clusters is analogous to the polyenes (aka polyboroenes), while the σ conjugation plays an equally important role in rendering the stability of the nanoribbons. The concept of σ conjugation established here has no analogues in hydrocarbons. Calculations suggest the viability of even larger boronyl polyboroenes, $B_{16}(BO)_2$ and $B_{20}(BO)_2$, extending the boron nanoribbons to ~1.5 nm in length or possibly even longer. The nanoribbons form a new class of nanowires and may serve as precursors for a variety of boron nanostructures. © *2013 AIP Publishing LLC*. [http://dx.doi.org/10.1063/1.4827501]

I. INTRODUCTION

Joint experimental and computational studies over the past decade have shown that elemental boron clusters possess planar or quasi-planar structures up to unusually large sizes,[1–11] in contrast to bulk boron where three-dimensional (3D) icosahedral B_{12} cage units dominate.[12–14] The planar or quasi-planar boron clusters exhibit great structural diversities, featuring in-plane hypercoordination,[1] circular and elongated geometries,[2,6] and concentric dual-ring structures,[8] which has been considered as a molecular Wankel motor.[15] It has been established that such structural diversities are a result of the intrinsic electron deficiency of boron, giving rise to π and σ aromaticity/antiaromaticity.[1–4,16–18] The π bonding in boron clusters is further shown to resemble that in the aromatic hydrocarbons, leading to the concept of hydrocarbon analogues of boron clusters.[1,2,6–8,11] Doping boron clusters can yield new species with tunable structural and electronic properties.[19–25] Among recent works in this direction are the studies on boron dihydride clusters.[26,27] Using photoelectron spectroscopy (PES) and density-functional theory (DFT) calculations, Wang and co-workers[26] have produced and characterized a series of $B_nH_2^-$ ($n = 7-12$) clusters. Independently, Li and co-workers[27] carried out DFT calculations on a series of boron dihydride clusters including B_4H_2, B_8H_2, $B_{12}H_2$, and their anions. These works concluded that $B_nH_2^-$ and B_nH_2 clusters possess planar, elongated, ladder-like double-chain structures terminated by a hydrogen atom on each end. It was shown that in these dihydride species a rhombic B_4 unit, which effectively contributes two delocalized π electrons, appears to be equivalent to a C=C unit in polyenes. This establishes an interesting analogy between boron dihydride clusters and the conjugated polyenes, and polyboroene was coined to designate this new class of boron compounds.[26]

Boronyl (BO) has a strong B≡O triple bond[28–30] comparable to that in CN. Recent studies have shown that BO group dominates the electronic and structural properties of boron-rich oxide clusters.[31–34] BO as a monovalent σ radical is analogous to H, suggesting a new route to design novel boron oxide clusters. In particular, the boron dioxide clusters, $B_{n+2}O_2^-$ or $B_{n+2}O_2$, are expected to be isolobal to the $B_nH_2^-$ or B_nH_2 clusters.[26,27] Here we report the observation and characterization of a series of boron dioxide clusters, $B_xO_2^-$ ($x = 7-14$), using PES and theoretical calculations. These dioxide clusters and their corresponding neutrals are shown to possess elongated double-chain structures with two boronyl groups attached terminally and can be formulated as $B_n(BO)_2^-$ and $B_n(BO)_2$ ($n = 5-12$). Theoretical calculations further suggest that even larger elongated boron dioxide clusters are possible, such as $B_{16}(BO)_2$ and $B_{20}(BO)_2$. The electron affinities (EA) of $B_n(BO)_2$ are found to follow a $4n$ periodic pattern, indicating the rhombic B_4 unit as the building block in the boron nanoribbons. Both π and σ conjugations are found in these nanoribbon clusters, which is not known in hydrocarbon molecules. It is noted that the double-chain boron nanoribbons are the favored structural features in a variety of proposed low-dimensional boron nanostructures, such as the tubular boron clusters,[3,5] the B_{80} fullerene,[35] and the most stable form of monolayer boron sheet.[36–40]

a)Electronic addresses: hj.zhai@sxu.edu.cn and lisidian@sxu.edu.cn.
b)Electronic mail: lai-sheng_wang@brown.edu.

II. METHODS

A. Photoelectron spectroscopy

The experiment was carried out using a magnetic-bottle PES apparatus equipped with a laser vaporization cluster source, details of which were described in Ref. 41. Briefly, $B_xO_y^-$ clusters were produced using a disk target made of enriched ^{10}B isotope (99.75%) in the presence of a helium carrier gas seeded with 0.01% O_2 and analyzed using a time-of-flight mass spectrometer. The $B_xO_2^-$ ($x = 7-14$) species were each mass-selected and decelerated before being photodetached. The PES spectra were obtained at 193 nm (6.424 eV) from an ArF excimer laser. PES data at 266 nm (4.661 eV) from an Nd:YAG laser were also obtained (mostly not shown) and were used to obtain more accurate binding energies. The PES spectra were calibrated using the known spectra of Au^- and Rh^-, and the resolution of the apparatus was $\Delta E_k/E_k \approx 2.5\%$, that is, ~25 meV for 1 eV kinetic energy electrons.

B. Computational methods

The DFT calculations were carried out at the hybrid B3LYP level[42] with the 6-311++G(d,p) basis sets.[43] Vibrational analyses were performed to confirm that all double-chain $B_n(BO)_2^-$ and $B_n(BO)_2$ ($n = 4-12$) clusters are true minima. Electronic excitation energies of the neutral clusters were calculated using the time-dependent DFT (TDDFT) method[44,45] at the anion ground-state geometries. Single-point CCSD(T) calculations[46–48] were done using the same basis sets at the B3LYP geometries to further refine the ADEs and VDEs. All calculations were performed using the Gaussian 09 package.[49] Molecular orbitals were visualized using Molekel 4.3.[50]

III. RESULTS

A. Experimental results

The PES spectra of $B_xO_2^-$ ($x = 7-14$) are shown in Fig. 1. The ground state adiabatic (ADE) and vertical (VDE) detachment energies are given in Table I. The ground state ADE that defines the EA of the neutral cluster is obtained from the 0–0 transition for the vibrationally resolved ground state band X. For those spectra without vibrational resolution, the ADEs are evaluated by drawing a straight line along the leading edge of band X and then adding the instrumental resolution to the intersection with the binding energy axis. Higher VDEs are given in Tables SI and SII in the supplementary material,[51] where they are compared with the theoretical data.

All PES spectral features observed for $B_xO_2^-$ ($x = 9-14$) are remarkably similar to those reported previously for the corresponding dihydrides,[26] $H_2B_n^-$ ($n = 7-12$), respectively, except that the electron binding energies of the dihydrides are lower by ~1 eV. The spectral similarities suggest that the $B_xO_2^-$ clusters should have similar structures as the dihydrides and should be formulated as $B_n(BO)_2^-$ with two boronyl groups as σ radicals. The EA of BO is much higher than that of the H atom.[30,52] Hence, the BO σ radical should be much more electron-withdrawing relative to the H atom, resulting in much higher electron binding energies observed for the oxides. Vibrationally resolved PES bands are observed for a number of species, that is, the X band for $B_8O_2^-$ and $B_9O_2^-$ and the A band for $B_{12}O_2^-$ and $B_{13}O_2^-$, yielding symmetric vibrational frequencies for their corresponding neutrals, which are compared with the calculated values in Table SIII.[51] Weakly populated isomers are clearly observed in the cases of $B_{12}O_2^-$ (the X′ feature in Fig. 1(f)) and $B_{14}O_2^-$ (the X′ feature in Fig. 1(h)). As will be shown below, the intense A and B bands observed for $B_{11}O_2^-$ (Fig. 1(e)) are also due to a nearly degenerate isomer (Table SII and Fig. S1).[51] Interestingly, even the spectral features from the isomers are similar to those observed for the corresponding $B_nH_2^-$ species,[26] suggesting that the diboronyl and dihydride boron clusters have similar potential landscapes.

B. Theoretical results

As already hinted by the PES spectra, we initially only optimized a set of structures at the B3LYP/6-311++G(d,p) level for the boron dioxide anion clusters with two boronyls, $B_n(BO)_2^-$ ($n = 5-12$), as shown in Fig. 2, which are analogous to the ladder-like $B_nH_2^-$ clusters. The $B_4(BO)_2^-$ cluster was studied previously[53] and is included here for comparison. Similar structures for the $B_n(BO)_2$ neutral species were also optimized and are given in Fig. S2.[51] The diboronyl type of structures for the boron dioxide clusters were also reported for $n = 5-8$ in a previous computational study.[34] For $B_9(BO)_2^-$, we considered a variety of structures based on two BO units bonded to different positions on the B_9 molecular wheel (Fig. S1).[1,51] One structure based on a distorted B_9 wheel with C_1 symmetry was found to be competitive with the double-chain C_2 structure, within ~1 kcal/mol at the single-point CCSD(T)//B3LYP/6-311++G(d,p) level. Nonetheless, their calculated first VDE values are very different from each other, 4.59 eV for C_1 versus 3.98 eV for C_2 at the B3LYP level (Table SII),[51] which ensure that such isomeric structures can be easily identified without ambiguity in the PES spectrum. All double-chain ladder-like $B_n(BO)_2^-$ and $B_n(BO)_2$ clusters adopt planar structures with D_{2h}, C_{2h}, or C_{2v} symmetries, except for $B_5(BO)_2^-$ and $B_9(BO)_2^-$, which undergo slight out-of-plane distortion, resulting in C_2 symmetry. The out-of-plane distortion of $B_9(BO)_2^-$ is exactly the same as that found in $B_9H_2^-$.[26] For even n clusters, the two BO groups are in *trans* positions, whereas for odd n clusters they are in *cis* positions, similar to the dihydrides. Several alternative anion and neutral structures (not shown) were also considered for all $B_n(BO)_2^-$ and $B_n(BO)_2$ ($n = 5-12$) clusters. As mentioned above, the isolobal analogy between the diboronyls and dihydrides and the similarity between the PES spectra of the dioxides and the dihydrides allowed us to bypass extensive structural searches usually necessary to find the global minima for such complicated systems.

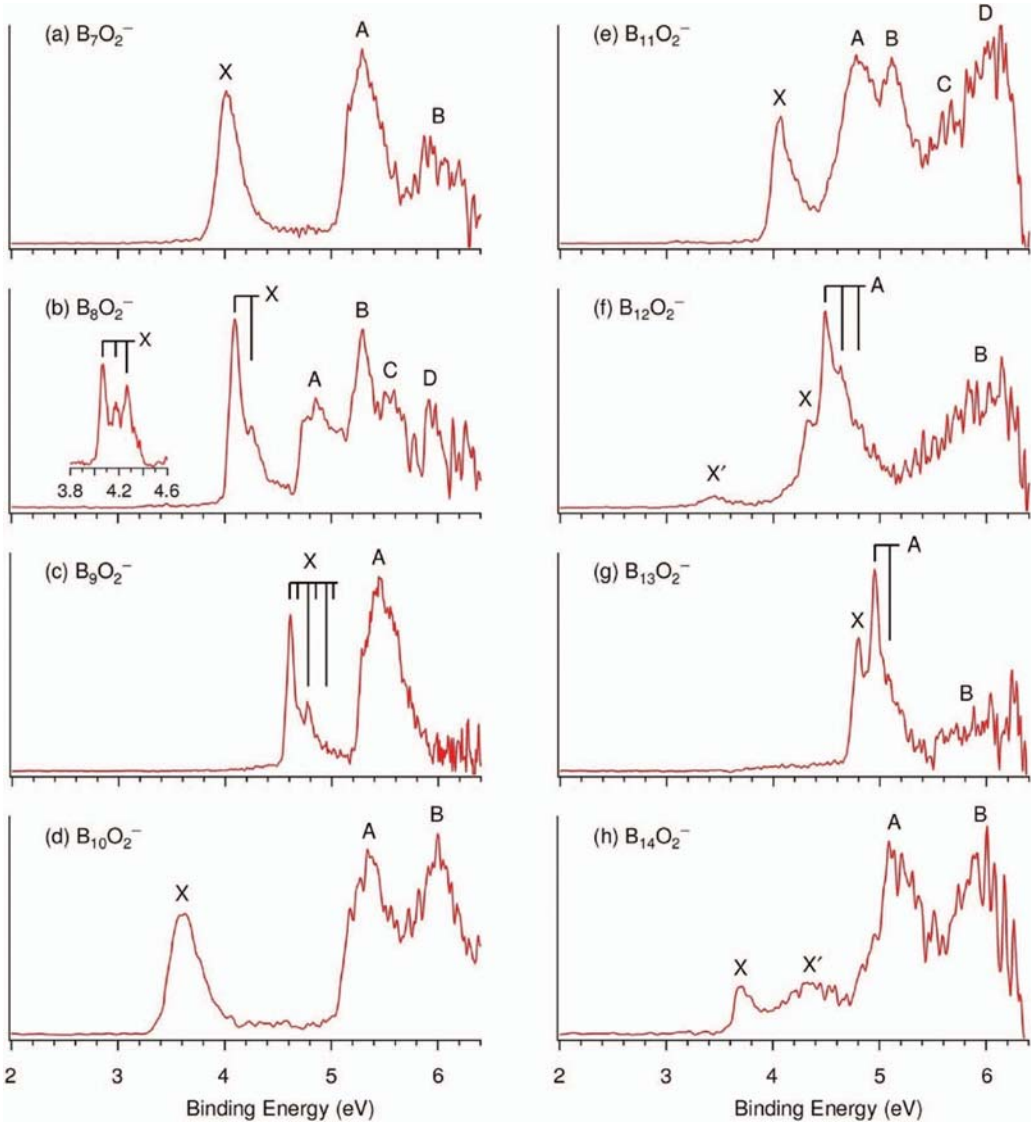

FIG. 1. Photoelectron spectra of $B_xO_2^-$ ($x = 7-14$) at 193 nm (6.424 eV). Vertical lines represent vibrational structures. The inset in (b) shows the spectrum at 266 nm (4.661 eV).

TABLE I. Experimental ground state adiabatic (ADE) and vertical (VDE) detachment energies from the photoelectron spectra of $B_xO_2^-$ ($x = 7-14$), compared to theoretical calculations. All energies are in eV.

Species	ADE (expt.)[a,b]	VDE (expt.)[a]	Transition	ADE (theor.)[c]	VDE (theor.)[c]
$B_7O_2^-$	3.90 (3)	4.01 (3)	$^2A_1 \leftarrow {}^1A$	3.69/***3.61***	3.89/***3.82***
$B_8O_2^-$	4.07 (2)	4.07 (2)	$^1A_g \leftarrow {}^2B_g$	4.12/***3.87***	4.21/***3.99***
$B_9O_2^-$	4.61 (3)	4.61 (3)	$^2A_2 \leftarrow {}^1A_1$	4.50/***4.42***	4.60/***4.57***
$B_{10}O_2^-$	3.50 (5)	3.62 (5)	$^1A_g \leftarrow {}^2B_u$	3.56/***3.31***	3.71/***3.42***
$B_{11}O_2^-$	3.98 (5)	4.06 (5)	$^2B_2 \leftarrow {}^1A$	3.86/***3.80***	3.98/***3.90***
	4.45 (5)[d]	4.81 (5)[d]	$^2A \leftarrow {}^1A$	4.22/***4.22***[d]	4.59/***4.58***[d]
$B_{12}O_2^-$	4.33 (3)	4.33 (3)	$^1A_g \leftarrow {}^2A_u$	4.28/***4.07***	4.39/***4.23***
$B_{13}O_2^-$	4.80 (3)	4.80 (3)	$^2B_1 \leftarrow {}^1A_1$	4.65/***4.60***	4.74/***4.76***
$B_{14}O_2^-$	3.67 (5)	3.72 (5)	$^1A_g \leftarrow {}^2A_g$	3.68/***3.47***	3.78/***3.53***

[a]Numbers in the parentheses represent experimental uncertainties in the last digit.
[b]Electron affinity of the neutral species.
[c]Calculated at the B3LYP/6-311++G(d,p) level. Shown in bold italic are values calculated at the single-point CCSD(T)//B3LYP/6-311++G(d,p) level.
[d]Coexisting isomer.

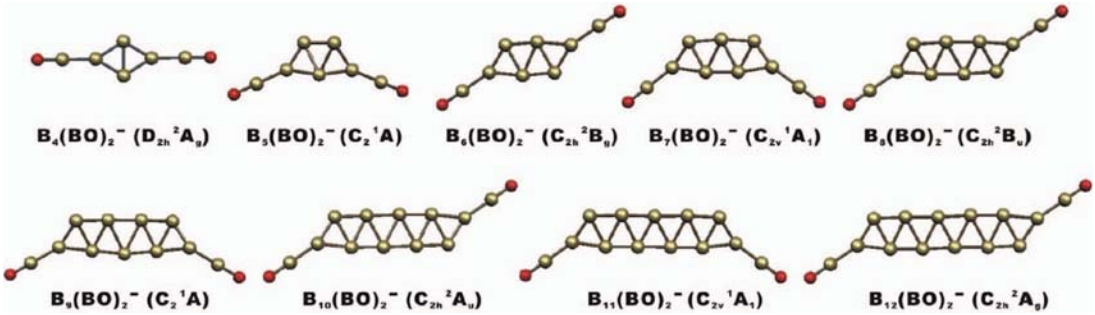

FIG. 2. Optimized double-chain nanoribbon global-minimum structures for $B_n(BO)_2^-$ ($n = 4-12$).

IV. COMPARISON BETWEEN EXPERIMENT AND THEORY

The calculated ground state ADEs and VDEs for $B_n(BO)_2^-$ ($n = 5-12$), at both the B3LYP/6-311++G(d,p) and single-point CCSD(T)//B3LYP/6-311++G(d,p) levels, are compared with the experimental data in Table I. The B3LYP results are in good agreement with the experimental data, with errors of less than ~0.2 eV. Indeed, for the majority of these values, the B3LYP results are within ~0.1 eV of the experimental data. The single-point CCSD(T) values are slightly lower than those at B3LYP in most cases, which are also in overall good agreement with experiment within ~0.1 eV. It may be stated that the B3LYP and single-point CCSD(T) methods perform equally well for the current system. More detailed comparisons of the calculated excited-state transitions with the experiment are given in Tables SI and SII.[51] The experimental VDEs can be viewed as the electronic fingerprint of a cluster. The double-chain nanoribbon structures shown in Fig. 2 reproduce well the experimental PES patterns for all the $B_n(BO)_2^-$ ($n = 5-12$) clusters, confirming these structures as their global minima. The experimentally resolved vibrational frequencies are compared with the calculated symmetric modes for the neutral ground state structures in Table SIII,[51] showing also good agreement between experiment and theory.

The VDEs for the first and second detachment channels from the second isomer of $B_9(BO)_2^-$ (C_1; Fig. S1 and Table SII)[51] are also in excellent agreement with the observed A and B bands (Fig. 1(e)), whereas the VDEs for the C_2 ribbon structure are in good agreement with the remaining spectral features. The second detachment channel of the C_2 $B_9(BO)_2^-$ corresponds to band C, giving rise to a large energy gap between the first and second detachment channels, resembling exactly the spectral features for $B_9H_2^-$.[26] As discussed for the $B_9H_2^-$ case, the large gap for $B_9(BO)_2^-$ suggests that its HOMO is relatively unstable, which causes the out of plane distortion. Removing the two electrons should result in a much more stable and perfectly planar $B_9(BO)_2^+$ species, similar to $B_9H_2^+$.[26] The much weakly populated isomers for $B_{10}(BO)_2^-$ and $B_{12}(BO)_2^-$ are also similar to those of the corresponding dihydrides. The overall excellent agreement between the calculated and experimental data lends strong support for the nanoladder structures of the boron dioxide clusters, which provide new examples for the BO/H isolobal analogy.

V. DISCUSSION

A. Chemical bonding in boron nanoribbons: π conjugation in $B_n(BO)_2^-$ and $B_n(BO)_2$ and analogy to polyenes

The experimental and theoretical EAs of $B_n(BO)_2$ and B_nH_2 ($n = 4-12$) are displayed in Fig. 3, revealing a regular $4n$ periodicity. This observation suggests that the rhombic B_4 unit plays an essential role in the double-chain nanoribbon structures. In particular, the low EAs for B_4X_2, B_8X_2, and $B_{12}X_2$ (X = H and BO) concur with their large HOMO-LUMO gaps, indicating highly stable neutral species. The chemical bonding in the $B_n(BO)_2^-$ and $B_n(BO)_2$ nanoribbons can be elucidated through MO analyses (Figs. 4 and S3)[51] and adaptive natural density partitioning (AdNDP) analyses (Fig. 5).[54] We found that, similar to the corresponding dihydrides, the $B_4(BO)_2$, $B_8(BO)_2$, and $B_{12}(BO)_2$

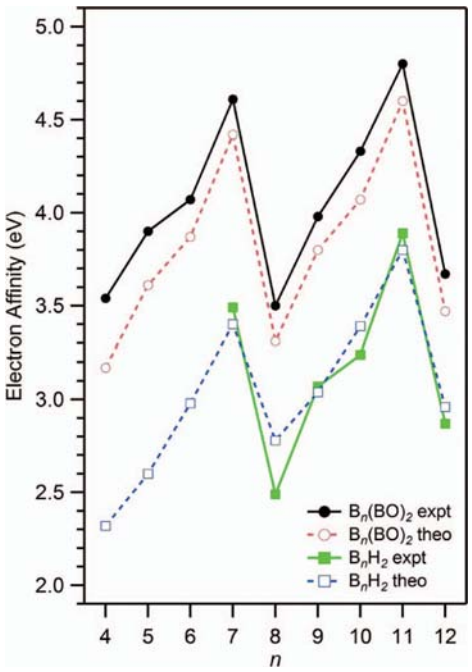

FIG. 3. The experimental electron affinities of $B_n(BO)_2$ ($n = 4-12$; solid dots) as a function of n, compared to theoretical values at the single-point CCSD(T)//B3LYP/6-311++G(d,p) level (empty dots). The EA of $B_4(BO)_2$ is taken from Ref. 53. Computational ground-state vertical detachment energies of $B_nH_2^-$ at the B3LYP level (empty squares, Ref. 27) and experimental values (solid squares, Ref. 26) are also shown for comparison.

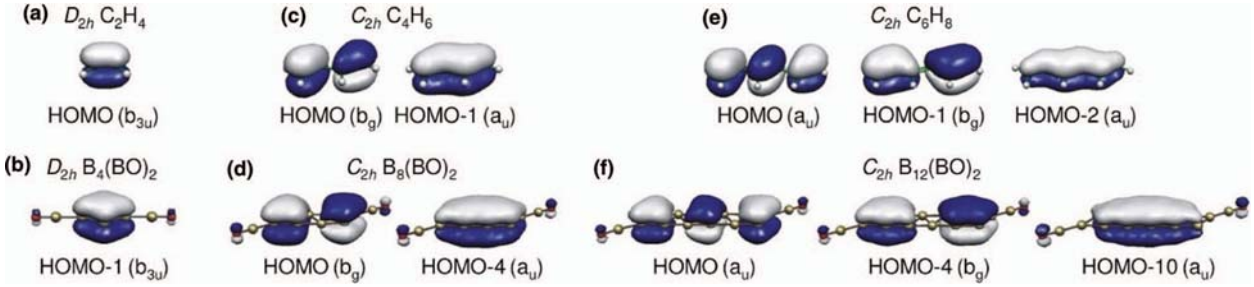

FIG. 4. Comparison of the delocalized π molecular orbitals of (a) C_2H_4 and (b) $B_4(BO)_2$, (c) C_4H_6 and (d) $B_8(BO)_2$, and (e) C_6H_8 and (f) $B_{12}(BO)_2$.

nanoribbons possess one, two, and three delocalized π MOs, respectively, which resemble those in ethylene, 1,3-butadiene, and 1,3,5-hexatriene (Fig. 4). Therefore, these boron dioxide clusters can be considered as boronyl analogues of the conjugated polyenes, similar to the bonding revealed recently in the $B_nH_2^-/B_nH_2$ clusters.[26,27] Polyboroenes have been coined for the boron dihydride nanoribbons.[26] Hence, the dioxides are boronyl polyboroenes, where the rhombic B_4 unit is equivalent to a C=C unit in the polyenes.

Figure 5 presents the AdNDP analyses for all the closed-shell neutral and anionic species of the boron dioxide nanoribbons for $n = 4-12$. The AdNDP represents the bonding of a molecule in terms of n-center two-electron (nc-2e) bonds, with n ranging from one to the total number of atoms in the molecule.[54] AdNDP thus recovers the classical Lewis bonding elements (lone pairs and 2c-2e bonds), as well as the nonclassical nc-2e delocalized bonds. As in pure boron clusters,[1–11] the B−B bonds in the periphery in the nanoribbons are described by 2c-2e bonds, whereas the bonding between the two boron rows in the nanoribbons is via delocalized σ and π bonds. As shown in Fig. 5, the delocalized π bonds are over B_4 rhombus units in $B_4(BO)_2$, $B_8(BO)_2$, and $B_{12}(BO)_2$. Other nanoribbons at different charge states exhibit similar π bonding patterns as these three prototypical polyboroenes.

B. σ conjugation in polyboroenes

The delocalized σ bonds in the $B_n(BO)_2^-$ clusters (Figs. 5 and S3)[51] are similar to the delocalized π bonds, suggesting σ conjugation in the boronyl polyboroenes, in addition to the π conjugation. There are no known cases of σ conjugation in hydrocarbon molecules. Thus, the σ conjugation in the polyboroenes is quite unique as a new bonding feature. As shown in Fig. 5, the partition of the π or σ bonds alters, depending on the size and the charge state of the boronyl polyboroenes. In the ideal cases when the number of π bonds differs from that of σ bonds, such as in $B_8(BO)_2$ and $B_{12}(BO)_2$, the π and σ bonds are delocalized over alternating B_4 units in the boron ribbon framework, giving rise to a more balanced bonding pattern throughout the nanoribbons. This bonding pattern results in the highly stable $B_8(BO)_2$ and $B_{12}(BO)_2$ boronyl polyboroenes. In cases when the number of π bonds is equal to that of the σ bonds, the π and σ bonds are delocalized over the same B_4 unit, as seen in $B_6(BO)_2$ and $B_{10}(BO)_2$ (Fig. 5). This bonding pattern gives rise to more

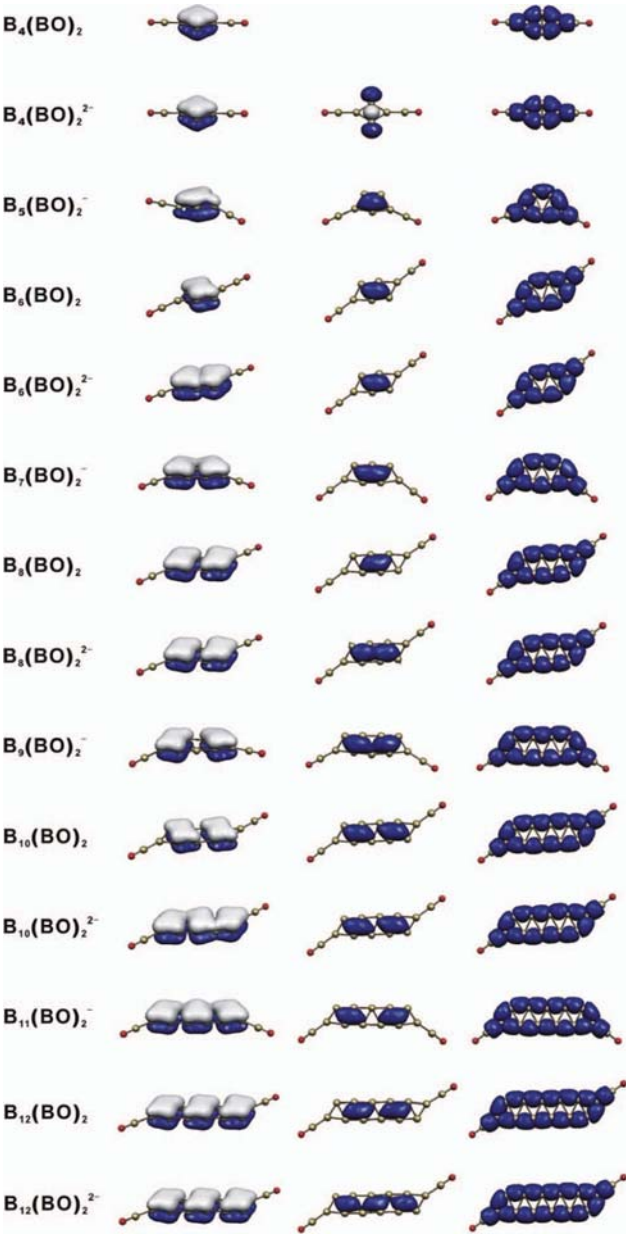

FIG. 5. AdNDP analyses for closed-shell $B_n(BO)_2$, $B_n(BO)_2^-$, and $B_n(BO)_2^{2-}$ ($n = 4-12$). For odd n species, monoanions are considered, whereas for even n species both neutrals and dianions are analyzed. Only the bonds within the B_n nanoribbon frameworks are shown; the localized bonding elements within the BO groups are not shown. Left column: delocalized π bonds; middle column: delocalized σ bonds; right column: peripheral two-center two-electron σ bonds.

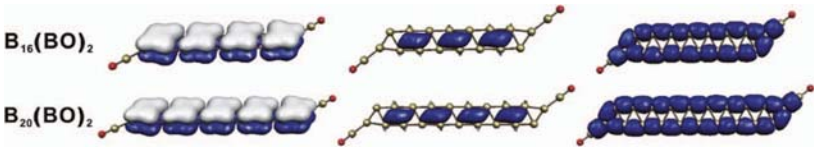

FIG. 6. AdNDP analyses for the boronyl polyboroenes, $B_{16}(BO)_2$ and $B_{20}(BO)_2$. The localized bonding elements within the BO groups are not shown. Left column: delocalized π bonds; middle column: delocalized σ bonds; right column: peripheral two-center two-electron σ bonds.

strongly bonded versus less bonded B_4 units and can result in structural distortions along the nanoribbon.

C. Possibility for larger polyboroenes

We note that the double-chain nanoribbon structures are also the key structural elements in the proposed B_{80} cage[35] and the 2D boron sheets.[36] Therefore, much longer polyboroenes terminated by BO may be possible. The strong electron-withdrawing capability of BO relative to H hints that boronyl polyboroenes should be more stable than the hydride polyboroenes. In the boronyl polyboroenes, the intramolecular Coulomb repulsion between two BO groups offers a driving force to elongate the clusters to the nanoribbon shapes. Furthermore, the π orbitals in the terminal BO groups can also participate in the π conjugation in the nanoribbon clusters, thus providing additional stabilization to the nanoribbon system.

As suggested by the $4n$ periodicity (Fig. 3), the next expected stable boronyl polyboroenes should be $B_{16}(BO)_2$ and $B_{20}(BO)_2$. We thus carried out preliminary calculations at the B3LYP level and found that these two nanoribbons are indeed highly stable among the alternative structures located in our structural searches (Fig. S4).[51] The $B_{20}(BO)_2$ boronyl polyboroene is about ~1.5 nm in length. The delocalized MOs of these two boronyl polyboroenes are given in Fig. S5 in the supplementary material[51] and their AdNDP bonding patterns are shown in Fig. 6. Thus, $B_{16}(BO)_2$ and $B_{20}(BO)_2$ are boronyl analogues of the larger polyenes, $H(CH{=}CH)_nH$ ($n = 4, 5$), respectively.

VI. CONCLUSIONS

A series of boron dioxide clusters, $B_n(BO)_2^-$ and $B_n(BO)_2$ ($n = 5{-}12$), are produced and characterized via photoelectron spectroscopy and quantum chemical calculations. The electron affinities of $B_n(BO)_2$ display a $4n$ periodicity, implying that the rhombic B_4 unit is the natural structural building block in the boron dioxide clusters. These clusters are shown to possess double-chain nanoribbon structures with lengths ranging from 2.7 to 8.9 Å, with the two boronyl groups bonded at each end. The π bonding in these nanoribbons is analogous to polyenes and they thus belong to a new class of boronyl polyboroenes. Preliminary theoretical calculations suggest that even larger boronyl polyboroenes, $B_{16}(BO)_2$ and $B_{20}(BO)_2$, are viable, extending the nanoribbon length to ~1.5 nm. These clusters may be viewed as molecular zippers, in which two boron atomic-chains are bonded together via π and σ double conjugations, a unique bonding feature unknown in hydrocarbons. The new boron nanoribbons may serve as novel molecular wires, as well as precursors for low-dimensional boron nanostructures.

ACKNOWLEDGMENTS

This work was supported by the US National Science Foundation (CHE-1263745 to L.-S.W.) and the National Natural Science Foundation of China (Grant Nos. 21243004 and 21373130). H.-J.Z. gratefully acknowledges the start-up fund from Shanxi University for support.

[1] H. J. Zhai, A. N. Alexandrova, K. A. Birch, A. I. Boldyrev, and L. S. Wang, Angew. Chem., Int. Ed. **42**, 6004 (2003).
[2] H. J. Zhai, B. Kiran, J. Li, and L. S. Wang, Nature Mater. **2**, 827 (2003).
[3] B. Kiran, S. Bulusu, H. J. Zhai, S. Yoo, X. C. Zeng, and L. S. Wang, Proc. Natl. Acad. Sci. U.S.A. **102**, 961 (2005).
[4] A. N. Alexandrova, A. I. Boldyrev, H. J. Zhai, and L. S. Wang, Coord. Chem. Rev. **250**, 2811 (2006).
[5] E. Oger, N. R. M. Crawford, R. Kelting, P. Weis, M. M. Kappes, and R. Ahlrichs, Angew. Chem., Int. Ed. **46**, 8503 (2007).
[6] A. P. Sergeeva, D. Yu. Zubarev, H. J. Zhai, A. I. Boldyrev, and L. S. Wang, J. Am. Chem. Soc. **130**, 7244 (2008).
[7] A. P. Sergeeva, B. B. Averkiev, H. J. Zhai, A. I. Boldyrev, and L. S. Wang, J. Chem. Phys. **134**, 224304 (2011).
[8] W. Huang, A. P. Sergeeva, H. J. Zhai, B. B. Averkiev, L. S. Wang, and A. I. Boldyrev, Nature Chem. **2**, 202 (2010).
[9] Z. A. Piazza, W. L. Li, C. Romanescu, A. P. Sergeeva, L. S. Wang, and A. I. Boldyrev, J. Chem. Phys. **136**, 104310 (2012).
[10] C. Romanescu, D. J. Harding, A. Fielicke, and L. S. Wang, J. Chem. Phys. **137**, 014317 (2012).
[11] A. P. Sergeeva, Z. A. Piazza, C. Romanescu, W. L. Li, A. I. Boldyrev, and L. S. Wang, J. Am. Chem. Soc. **134**, 18065 (2012).
[12] N. N. Greenwood and A. Earnshaw, *Chemistry of the Elements*, 2nd ed. (Butterworth-Heinemann, Oxford, 1997).
[13] A. R. Oganov, J. H. Chen, C. Gatti, Y. Z. Ma, Y. M. Ma, C. W. Glass, Z. X. Liu, T. Yu, O. O. Kurakevych, and V. L. Solozhenko, Nature (London) **457**, 863 (2009).
[14] T. Ogitsu, F. Gygi, J. Reed, Y. Motome, E. Schwegler, and G. Galli, J. Am. Chem. Soc. **131**, 1903 (2009).
[15] J. O. C. Jiménez-Halla, R. Islas, T. Heine, and G. Merino, Angew. Chem., Int. Ed. **49**, 5668 (2010).
[16] J. E. Fowler and J. M. Ugalde, J. Phys. Chem. A **104**, 397 (2000).
[17] J. I. Aihara, J. Phys. Chem. A **105**, 5486 (2001).
[18] J. I. Aihara, H. Kanno, and T. Ishida, J. Am. Chem. Soc. **127**, 13324 (2005).
[19] C. Romanescu, A. P. Sergeeva, W. L. Li, A. I. Boldyrev, and L. S. Wang, J. Am. Chem. Soc. **133**, 8646 (2011).
[20] W. L. Li, C. Romanescu, T. R. Galeev, L. S. Wang, and A. I. Boldyrev, J. Phys. Chem. A **115**, 10391 (2011).
[21] C. Romanescu, T. R. Galeev, W. L. Li, A. I. Boldyrev, and L. S. Wang, Angew. Chem., Int. Ed. **50**, 9334 (2011).
[22] T. R. Galeev, C. Romanescu, W. L. Li, L. S. Wang, and A. I. Boldyrev, Angew. Chem., Int. Ed. **51**, 2101 (2012).
[23] W. L. Li, C. Romanescu, T. R. Galeev, Z. Piazza, A. I. Boldyrev, and L. S. Wang, J. Am. Chem. Soc. **134**, 165 (2012).
[24] C. Romanescu, T. R. Galeev, A. P. Sergeeva, W. L. Li, L. S. Wang, and A. I. Boldyrev, J. Organomet. Chem. **721**, 148 (2012).
[25] C. Romanescu, T. R. Galeev, W. L. Li, A. I. Boldyrev, and L. S. Wang, Acc. Chem. Res. **46**, 350 (2013).
[26] W. L. Li, C. Romanescu, T. Jian, and L. S. Wang, J. Am. Chem. Soc. **134**, 13228 (2012).

[27]D. Z. Li, Q. Chen, Y. B. Wu, H. G. Lu, and S. D. Li, Phys. Chem. Chem. Phys. **14**, 14769 (2012).
[28]H. Bock, L. Cederbaum, W. von Niessen, P. Paetzold, P. Rosmus, and B. Solouki, Angew. Chem., Int. Ed. Engl. **28**, 88 (1989).
[29]H. Braunschweig, K. Radacki, and A. Schneider, Science **328**, 345 (2010).
[30]H. J. Zhai, L. M. Wang, S. D. Li, and L. S. Wang, J. Phys. Chem. A **111**, 1030 (2007).
[31]H. J. Zhai, S. D. Li, and L. S. Wang, J. Am. Chem. Soc. **129**, 9254 (2007).
[32]S. D. Li, H. J. Zhai, and L. S. Wang, J. Am. Chem. Soc. **130**, 2573 (2008).
[33]H. J. Zhai, J. C. Guo, S. D. Li, and L. S. Wang, ChemPhysChem **12**, 2549 (2011).
[34]T. B. Tai, M. T. Nguyen, and D. A. Dixon, J. Phys. Chem. A **114**, 2893 (2010).
[35]N. G. Szwacki, A. Sadrzadeh, and B. I. Yakobson, Phys. Rev. Lett. **98**, 166804 (2007).
[36]H. Tang and S. Ismail-Beigi, Phys. Rev. Lett. **99**, 115501 (2007).
[37]X. Yang, Y. Ding, and J. Ni, Phys. Rev. B **77**, 041402 (2008).
[38]X. Wu, J. Dai, Y. Zhao, Z. Zhuo, J. Yang, and X. C. Zeng, ACS Nano **6**, 7443 (2012).
[39]E. S. Penev, S. Bhowmick, A. Sadrzadeh, and B. I. Yakobson, Nano Lett. **12**, 2441 (2012).
[40]H. G. Lu, Y. W. Mu, H. Bai, Q. Chen, and S. D. Li, J. Chem. Phys. **138**, 024701 (2013).
[41]L. S. Wang, H. S. Cheng, and J. Fan, J. Chem. Phys. **102**, 9480 (1995).
[42]A. D. Becke, J. Chem. Phys. **98**, 5648 (1993); C. T. Lee, W. T. Yang, and R. G. Parr, Phys. Rev. B **37**, 785 (1988).
[43]R. Krishnan, J. S. Binkley, R. Seeger, and J. A. Pople, J. Chem. Phys. **72**, 650 (1980).
[44]M. E. Casida, C. Jamorski, K. C. Casida, and D. R. Salahub, J. Chem. Phys. **108**, 4439 (1998).
[45]R. Bauernschmitt and R. Ahlrichs, Chem. Phys. Lett. **256**, 454 (1996).
[46]J. Čížek, Adv. Chem. Phys. **14**, 35 (1969).
[47]G. E. Scuseria and H. F. Schaefer, J. Chem. Phys. **90**, 3700 (1989).
[48]R. J. Bartlett and M. Musial, Rev. Mod. Phys. **79**, 291 (2007).
[49]M. J. Frisch, G. W. Trucks, H. B. Schlegel *et al.*, GAUSSIAN 09, Revision A.2, Gaussian, Inc., Wallingford, CT, 2009.
[50]S. Portmann, MOLEKEL, version 4.3, CSCS/ETHZ, 2002.
[51]See supplementary material at http://dx.doi.org/10.1063/1.4827501 for detailed comparison of the observed and calculated electron binding energies for $B_xO_2^-$ ($x = 7$–14); observed vibrational frequencies for the neutrals; alternative optimized structures for $B_9O_2^-$; optimized neutral double-chain structures for $B_n(BO)_2$ ($n = 4$–12); delocalized π and σ molecular orbitals for $B_n(BO)_2^-$; optimized structures for $B_{16}(BO)_2$ and $B_{20}(BO)_2$; the delocalized π and σ molecular orbitals for $B_{16}(BO)_2$ and $B_{20}(BO)_2$; and complete citation of Ref. 49.
[52]K. R. Lykke, K. K. Murray, and W. C. Lineberger, Phys. Rev. A **43**, 6104 (1991).
[53]Q. Chen, H. J. Zhai, S. D. Li, and L. S. Wang, J. Chem. Phys. **137**, 044307 (2012).
[54]D. Y. Zubarev and A. I. Boldyrev, Phys. Chem. Chem. Phys. **10**, 5207 (2008).